Article:
Chen, J, Kong, Y, Wang, W et al. (6 more authors) (2016) Direct Water-phase Synthesis of Lead Sulfide Quantum Dots Encapsulated by β-Lactoglobulin for In Vivo Second Near Infrared Window Imaging with Reduced Toxicity. Chemical Communications, 52. pp. 4025-4028. ISSN 1359-7345

https://doi.org/10.1039/C6CC00099A

COMMUNICATION

Direct Water-phase Synthesis of Lead Sulfide Quantum Dots Encapsulated by β-Lactoglobulin for *In Vivo* Second Near Infrared Window Imaging with Reduced Toxicity

Received 00th January 20xx,
Accepted 00th January 20xx

DOI: 10.1039/x0xx00000x

www.rsc.org/

Jun Chen [a], Yifei Kong [b], Wei Wang [c], Hongwei Fang [d], Yan Wo [e], Dejian Zhou [b], Ziying Wu[a], Yunxia Li [a*] and Shiyi Chen [a*]

Compared to traditional fluorescence imaging in the visible and NIR-I regions (700-900 nm), second near infrared window (NIR-II, 1000-1400 nm)-based optical imaging offers reduced photon scattering, deeper tissue penetration and lower auto-fluorescence. Despite the excellent imaging capabilities, current NIR-II probes have not yet reached their full potential for biomedical imaging applications due to weak quantum yields, low water solubility and suboptimal biocompatibility. To address these factors, NIR-II fluorescent PbS quantum dots (QDs) encapsulated by β-lactoglobulin (LG) are conveniently prepared via a one-pot microwave-assisted synthesis. The as-prepared LG-PbS QDs feature excellent aqueous dispersibility, high quantum yield and favorable biocompatibility. *In vivo* imaging experiments show that LG-PbS QDs are superbly suitable for real-time and high-resolution *in vivo* imaging; these features make these QDs extremely promising for use in various bioimaging applications.

Fluorescence-based optical imaging in the second near-infrared window (NIR-II, 1000-1400 nm) has become increasingly attractive due to the reduced photon scattering and almost zero autofluorescence from biological tissues, both of which benefit deep light penetration into the body with excellent image fidelity[1-4]. Simulations and modeling studies of optical imaging in blood and tissue have suggested that NIR-II emitters could effectively ameliorate the signal-to-noise ratios compared to their competitors that emit in the conventional first NIR window (NIR-I, 750-900 nm). Since then, myriad endeavors have been devoted to developing NIR-II probes, such as single-walled carbon nanotubes (SWNTs), organic molecules (e.g., polymer fluorophores[4]), inorganic quantum dots (QDs) (e.g., PbS [4-6], AgSe[7] and Ag_2S[8-10]) and rare-earth-doped nanoparticles[1, 11]. Among these, QDs display superior tunability, narrow emission, high quantum yield (QY) and robust photobleaching resistance; thus, they have attracted considerable attention in recent years due to their potential for use in imaging applications[3, 12]. However, certain obstacles, such as relatively low water solubility, sensitivity to biological microenvironments and potential toxicity, hinder the use of current NIR-II QDs for further biomedical applications. Therefore, much effort has been invested to address these problems.

Lead sulfide (PbS) is a IV-VI semiconductor with an extremely large bulk exciton Bohr radius of 20 nm[13], which creates strong quantum confinement in colloidal nanocrystals and allows their bandgap and absorption edge to be tuned from the visible region to the NIR region[14-17]. However, lead ions, a systemic toxicant, can adversely affect every organ system, especially the nervous system, and galena has an extremely low solubility product constant (K_{sp} = 3.4×10^{-28} mol^2•dm^{-6}), which guarantees minimum leakage of Pb^{2+} ions into biological surroundings [18]. Therefore, PbS QDs have been treated as a

[a] Department of Orthopedic Sports Medicine, Huashan Hospital, Fudan University, Shanghai 200040, China.
E-mail: liyunxia912@aliyun.com (Y.L.), cshiyi@163.com (S.C.); Tel&Fax: (+) 86-021-52888255.
[b] School of Chemistry and Astbury Structure for Molecular Biology, University of Leeds, Leeds LS2 9JT, UK.
[c] Department of Gastric and Pancreatic Surgery, Sun Yat-sen University Cancer Center, State Key Laboratory of Oncology in South China, Guangzhou 510060, China.
[d] Department of Anesthesiology, The First Affiliated Hospital of Bengbu Medical College, Anhui 233004, China.
[e] Department of Human Anatomy, Histology and Embryology,School of Medicine, Shanghai JiaoTong University, Shanghai 200025,China.
†Electronic Supplementary Information (ESI) available. See DOI: 10.1039/x0xx00000x

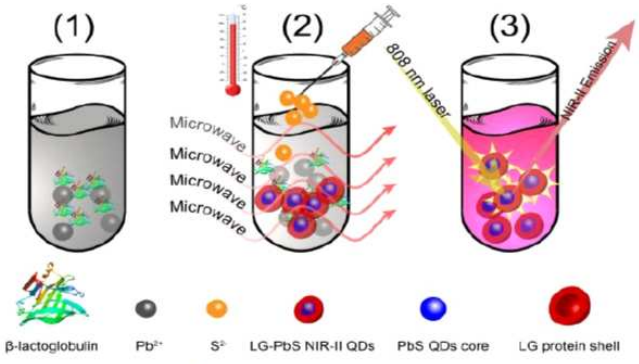

Scheme 1 Illustration of LG-PbS QD synthesis.

promising candidate for NIR imaging[19]. Recently, PbS QDs with NIR fluorescence emission have been successfully prepared using biomolecules such as DNA[5], apoferritin protein[20], luciferase enzyme[6] and glutathione (GSH) [21] as templates *via* a biometric route, significantly enhancing the stability of PbS QDs in either water solution or a biological microenvironment and decreasing the toxicity of PbS QDs by preventing the release of Pb ions from the "protective" protein layer coating the surface of the QDs. However, the above PbS QDs capped by biomolecules prepared in the water phase provided poor QYs under the NIR-II region, where the reported QYs are not more than 10% when the emission wavelength is above 1200 nm. Due to their low QYs, to the best of our knowledge, only one of these reported PbS QDs has been further demonstrated in *in vivo* NIR-II imaging[21]. Here, we report the direct water phase synthesis of PbS QDs encapsulated by β-lactoglobulin (LG) with emission in the NIR-II window *via* a microwave-assisted method, and the QDs exhibit a high photoluminescence (PL) response in the NIR-II window.

The globular protein β-lactoglobulin (LG), which contains 162 amino acids with an isoelectric point (pI) of 5.2 [22], is selected in this study because it has been widely developed for a long time for use in *in vivo* encapsulating systems for the delivery of nutrients[23], poorly water-soluble drugs [24-26] and, in more recent years, nanoparticles[27-29]. In this study, we expect LG to act as a stabilizer for the growth of PbS QDs in water and delivery in the blood circulation. Scheme 1 illustrates the synthetic route: **(1)** two precursors, $Pb(OAc)_2$ and LG, are mixed with deionized water in a reaction vessel prior to being placed in a microwave unit; **(2)** crystallization of the QDs is facilitated by microwave heating at 100 °C for 30 s under continuous stirring after the introduction of Na_2S; and **(3)** a solution of LG conjugated with NIR-II fluorescent PbS QDs (LG-PbS QDs) is eventually prepared.

In this synthetic route, temperature is the critical factor that determines the emission wavelength of the LG-PbS QDs. The emission of the LG-PbS QDs redshifts from 950 to 1400 nm with increasing reaction temperature (60, 80 or 100 °C). The QDs synthesized at 100 °C exhibited a higher luminescence intensity than the QDs synthesized at 60 °C and 80 °C (Fig.S1A). Interestingly, the luminescence intensity decreased significantly when the reaction temperature was greater than 100 °C. Moreover, different Pb^{2+} to S^{2-} ratios, including 10:1, 10:3 and 5:3, also led to different QYs from the LG-PbS QDs. These LG-PbS QDs generated the highest QY of 20.3% when the molar ratio of Pb^{2+}:S^{2-} was 5:3 (Fig.S1B), which was determined using IR-26 (QY = 0.5%) as a reference standard in this study. Thus, the as-synthesized LG-PbS QDs that exhibited NIR-II fluorescence with an emission peak at approximately 1300 nm and a QY of 20.3% were chosen for subsequent research (Fig.1A). The corresponding UV/vis absorption spectrum of the LG-PbS QDs is shown in Fig.1B. The result reveals that the LG-PbS QDs have stronger absorption in the long wavelengths from 300 nm to 500 nm compared to pure LG in that region, which is ascribed to the quantum effect of PbS QDs.

Fig.1C and D show the morphology of the as-prepared LG-PbS QDs observed by TEM and HR-TEM, respectively. The as-synthesized LG-PbS QDs are spherical in the TEM image (Fig.1C), and the HR-TEM image (Fig.1D) of an individual particle reveals its highly crystalline nature with an interplanar spacing of 0.295

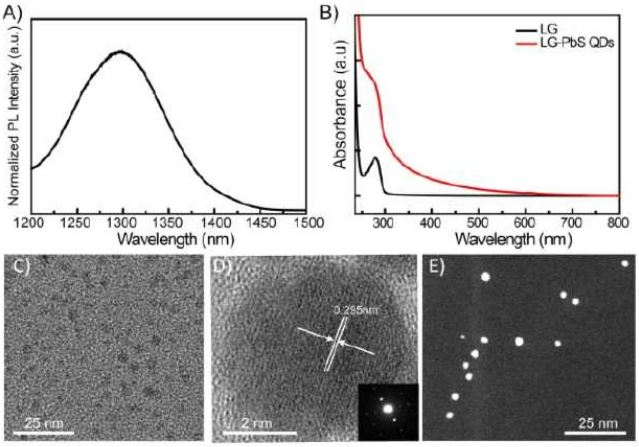

Fig.1 A) Photoluminescence spectrum of LG-PbS QDs. B) UV-vis absorption spectra of LG and LG-PbS QDs. C) TEM, D) HR-TEM and E) HDDF-STEM images of LG-PbS QDs. The inset in D) is the SAED pattern of a single PbS QD.

nm. However, the electron images of these LG-PbS QDs hardly allow the edges to be distinguished due to low bright-field contrast, adversely affecting their size measurements. Therefore, high angle annular dark field scanning TEM (HAADF-STEM) was utilized to obtain an incoherent image of the LG-PbS QDs in Z-contrast imaging mode. As shown in Fig.1E, PbS QDs are clearly observed as bright dots in the HAADF-STEM image, and corresponding size analysis results show that PbS QDs have an average diameter of 4.45±0.27 nm by measuring 100 particles (Fig.S2A). Furthermore, the mean hydrodynamic diameter (HD) of the as-prepared LG-PbS QDs is 5.91 nm, as measured by dynamic light scattering (DLS) (Fig. S2B).

Next, we proceeded to evaluate the biocompatibility of our products by incubating a human embryonic kidney cell line (293T) with various concentrations of the LG-PbS QDs for 24 h. Cell viabilities of 293T cells treated with different concentrations of LG-PbS QDs are shown in Fig.2, and it was found that no evident cell proliferation inhibition was induced by LG-PbS QDs in the tested concentration range from 0.25 to

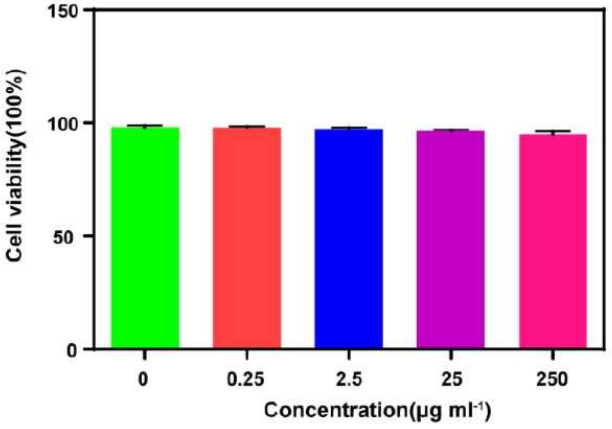

Fig.2 MTT analysis of 293T cells after incubation with various LG-Pb QD concentrations for 24 h.

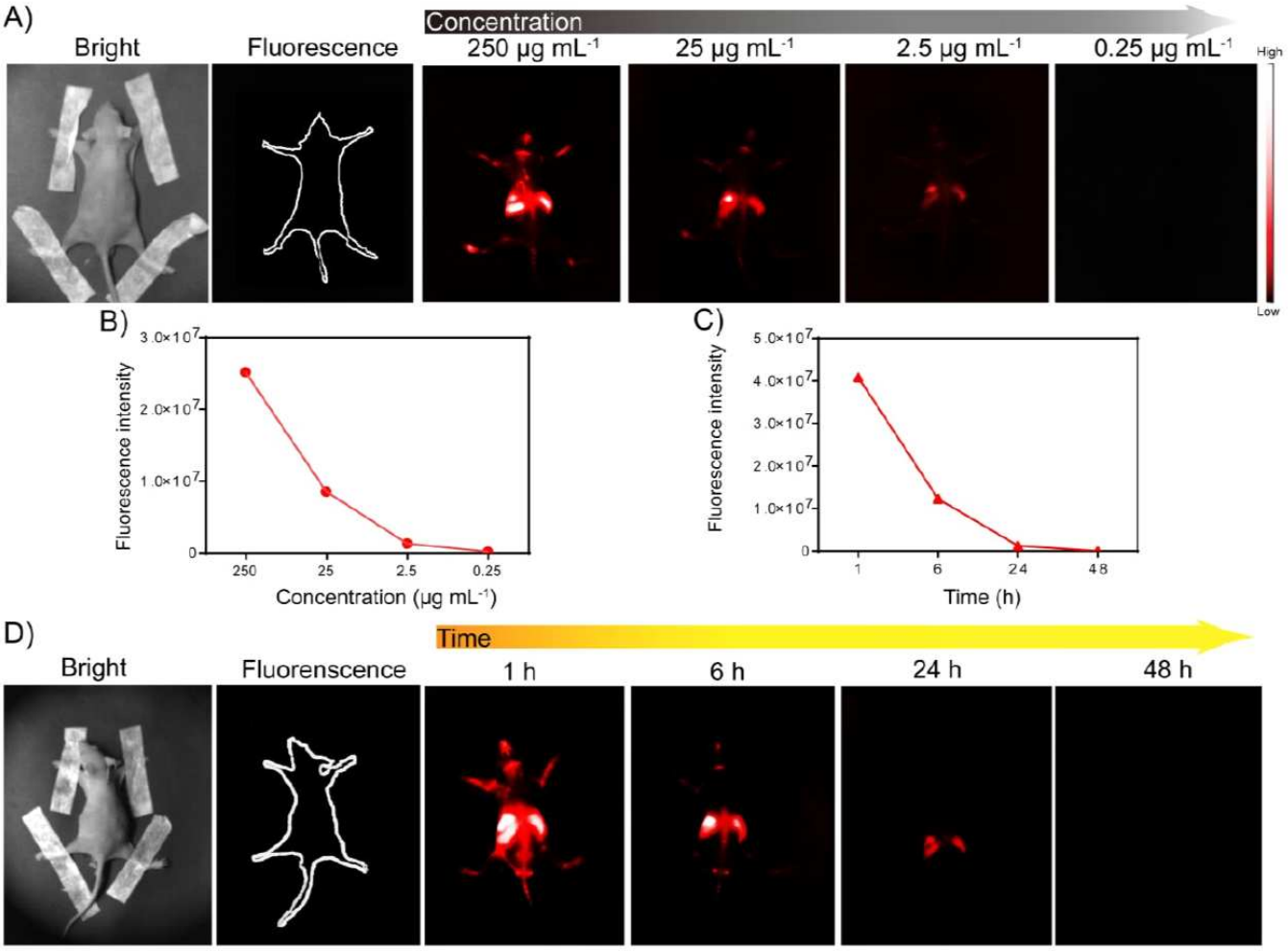

Fig.3 A) Comparison of the NIR-II fluorescence intensities of various LG-PbS QD concentrations (0.25, 2.5, 25 and 250 μg mL^{-1}) in nude mice 1 h after intravenous injection. B) Corresponding quantitative fluorescence intensity results at different concentrations. D) NIR-II images of 250 μg mL^{-1} LG-PbS QDs in the nude mice at different times (1 h, 6 h, 24 h and 48 h). C) Corresponding quantitative fluorescence intensity results at different time intervals.

25 μg ml^{-1} after 24 h of incubation. Moreover, flow cytometry analysis has been employed in order to further investigate these effects of our QDs for 293T cells. the corresponding results of cell distribution percentages indicate a growing tendency of the G0/G1 phase with increasing LG-PbS QD concentration compared to the control group (Fig.S3), and they only achieve statistical significance at the highest concentrations of QDs (250 μg ml^{-1}). The cell apoptosis and necrosis assays suggest that these treated groups induced by the QDs, even the concentration of QDs is 250 μg ml^{-1}, do not show a significant difference compared to the control group (Fig.S4). Moreover, the genotoxicity analysis confirms that our prepared LG-PbS QDs only induced a slight increase in the ratio of tail DNA (Fig.S5), indicating the low genotoxicity of LG-PbS QDs against normal cells. Based on these studies, we conclude that the LG-PbS QDs have good biocompatibility after the surface is coated with LG, which exerts limited effects on cell proliferation, differentiation and gene integrity.

To further evaluate the capability of as-prepared LG-PbS QDs for *in vivo* imaging, various concentrations of LG-PbS QDs were injected into nude mice via the tail vein and were observed under the same NIR-II imaging conditions. All photographs were taken using an exposure of 50 ms and 808-nm irradiation (6.5 W) 1 h after intravenous injection. As shown in Fig.3 A and B, the NIR-II fluorescence signals of our products were detected even at a low concentration of 2.5 μg mL^{-1}, which is ascribed to the high QY of the LG-PbS QDs and the ultra-low autofluorescence background of mice in the NIR-II region. Notably, mostly fluorescence signals of our products were located in the livers and spleens of the mice. Considering the depth of the livers and spleens of nude mice (3-5 mm), these results clearly demonstrate the advantages of our products for NIR-II *in vivo* imaging, including decreased photon scattering in biological tissues and improved signal-to-noise ratios for imaging [30], leading to higher spatial resolution at deeper tissue penetration depths.

A time-dependent *in vivo* imaging experiment was then conducted to further demonstrate the capabilities of our products for high-resolution and real-time imaging in the NIR-II region. *In vivo* images tracking the LG-PbS QDs at different time intervals are shown in Fig.3 C and D, and it is clear that the fluorescence intensity of the LG-PbS QDs gradually decreases

with increasing time. Specifically, the most important organs, such as the liver, spleen and lymph nodes, are clearly visualized at 1 h post-injection under 808-nm illumination. This result indicates that our products are rapidly distributed throughout the whole body of the mice via blood circulation. At 24 h post-injection, most of the QDs in the mice were cleared from most of the organs and blood, and only a small amount of LG-PbS QDs were detected in the liver and spleen, in agreement with that the metabolism of QDs is related to liver and spleen pathway[10]. The ex vivo analysis results confirm that most of the organs in mice are not visualized because our products are removed from them after 24 h, and only the liver and spleen are still detected (Fig.S6). Most of important, none of QDs' signals could be observed after 48 h post-injection, which suggests all of our products are rapidly clear out from body because of their ultra-small size. In addition, hematoxylin and eosin (H&E) staining was employed to investigate whether LG-PbS QDs would have any detrimental effects on these organs. The HE assay indicated that there were no significant notable lesions, inflammation, or other abnormalities in these main organs, including the spleen and liver (Fig.S7). These results illustrate that the toxicity of PbS QDs is negligible after coating with biocompatible and hydrophilic LG.

Conclusions

In summary, we have developed a microwave-assisted approach to synthesize highly NIR-II-emitting PbS QDs (QY=20.3%) in the aqueous phase using LG as a soft bio-template. Due to their surface coating with LG, the water-soluble LG-PbS QDs demonstrated good biocompatibility and ultra-low toxicity. The *in vivo* imaging studies illustrated that the resulting NIR-II QDs possess excellent capabilities for *in vivo* bioimaging with deep penetration and low detection thresholds. Our results highlight the promise of LG-PbS QDs as an NIR-II nanoprobe for high-resolution, real-time, noninvasive *in vivo* imaging, and further investigations are necessary to develop clinical applications in imaging-guided diagnosis and therapies.

Acknowledgements

This project was supported by the National 863 Hi-tech Project (2015AA033703), National Natural Science Foundation of China (No. 81271958, 81301672, 81401771 and 81201773), Natural Science Foundation of Shanghai Project (NO. 12ZR1415800 and NO.15ZR1405000), the Specialized Research Fund for the Doctoral Program of Higher Education (NO.20120071110067), China Postdoctoral Science Foundation (NO. 2014M560296) and Innovation Program of Shanghai Municipal Education Commission (NO.15ZZ006).

Notes and references

1. A. M. Smith, M. C. Mancini and S. Nie, *Nat. Nanotechnol.*, 2009, **4**, 710.
2. R. G. Aswathy, Y. Yoshida, T. Maekawa and D. S. Kumar, *Anal. Bioanal. Chem.*, 2010, **397**, 1417.
3. D. J. Naczynski, M. C. Tan, M. Zevon and B. Wall, *Nat. Commun.*, 2013, **4**, 1345.
4. G. Hong, Y. Zou, A. L. Antaris, S. Diao, D. Wu, K. Cheng, X. Zhang, C. Chen, B. Liu and Y. He, *Nat. Commun.*, 2014, **5**, 4206.
5. G. Hong, S. Diao, J. Chang, A. L. Antaris, C. Chen, B. Zhang, S. Zhao, D. N. Atochin, P. L. Huang and K. I. Andreasson, *Nat. Photonics*, 2014, **8**, 723.
6. L. Levina, V. Sukhovatkin, S. Musikhin, S. Cauchi, R. Nisman, D. P. Bazett-Jones and E. H. Sargent, *Adv. Mater.*, 2005, **17**, 1854.
7. N. Ma, A. F. Marshall and J. Rao, *J. Am. Chem. Soc.*, 2010, **132**, 6884.
8. B. Dong, C. Li, G. Chen, Y. Zhang, Y. Zhang, M. Deng and Q. Wang, *Chem. Mater.*, 2013, **25**, 2503.
9. Y. Du, B. Xu, T. Fu, M. Cai, F. Li, Y. Zhang and Q. Wang, *J. Am. Chem. Soc.*, 2010, **132**, 1470.
10. Y. Zhang, G. Hong, Y. Zhang, G. Chen, F. Li, H. Dai and Q. Wang, *ACS Nano*, 2012, **6**, 3695.
11. P. Jiang, Z. Q. Tian, C. N. Zhu, Z. L. Zhang and D. W. Pang, *Chem. Mater.*, 2011, **24**, 3.
12. R. Wang, X. Li, L. Zhou and F. Zhang, *Angew. Chem.*, 2014, **53**, 12086.
13. S. Kim, T. L. Yong, E. G. Soltesz, A. Grand, J. Lee, A. Nakayama, J. A. Parker, T. Mihaljevic, R. G. Laurence and D. M. Dor, *Nat. Biotechnol.*, 2004, **22**, 93.
14. F. W. Wise, *Acc. Chem. Res.*, 2000, **33**, 773.
15. I. Moreels, K. Lambert, D. Smeets, D. De Muynck, T. Nollet, J. C. Martins, F. Vanhaecke, A. Vantomme, C. Delerue, G. Allan and Z. Hens, *ACS Nano*, 2009, **3**, 3023.
16. M. A. Hines and G. D. Scholes, *Adv. Mater.*, 2003, **15**, 1844.
17. I. Kang and F. W. Wise, *J. Opt. Soc. Am. B: Opt. Phys.*, 1997, **14**, 1632.
18. C. B. Murray, S. Sun, W. Gaschler, H. Doyle, T. A. Betley and C. R. Kagan, *IBM J. Res. Dev.*, 2001, **45**, 47.
19. M. P. Beeston, J. T. V. Elteren, V. S. Šelih and R. Fairhurst, *Analyst*, 2009, **135**, 351.
20. P. M. Allen and M. G. Bawendi, *J. Am. Chem. Soc.*, 2008, **130**, 9240.
21. B. Hennequin, L. Turyanska, T. Ben, A. M. Beltrán, S. I. Molina, M. Li, S. Mann, A. Patanè and N. R. Thomas, *Adv. Mater.*, 2008, **20**, 3592.
22. Y. Nakane, Y. Tsukasaki, T. Sakata, H. Yasuda and T. Jin, *Chem. Commun.*, 2013, **49**, 7584.
23. M. Z. Papiz, L. Sawyer, E. E. Eliopoulos, A. C. T. North, J. B. C. Findlay, R. Sivaprasadarao, T. A. Jones, M. E. Newcomer and P. J. Kraulis, *Nature*, 1986, **324**, 383.
24. C. Lingyun and S. Muriel, *Biomaterials*, 2005, **26**, 6041-6053.
25. W. He, Y. Tan, Z. Tian, L. Chen and H. W. Wu, *Int. J. Nanomed.*, 2011, **6**, 521.
26. Y. Li, Z. Wu, W. He, C. Qin, J. Yao, J. Zhou and L. Yin, *Mol. Pharm.*, 2015, **12**, 1485.
27. W. He, K. Yang, L. Fan, Y. Lv, Z. Jin, S. Zhu, C. Qin, Y. Wang and L. Yin, *Int. J. Pharm.*, 2015, **495**, 9.
28. D. Xin, Z. Miao, Z. Di, Y. Fang, M. Min and C. Qiang, *Biosens. Bioelectron.*, 2014, **62**, 73.
29. X. Du, Z. Zhang, Z. Miao, M. Ma, Y. Zhang, C. Zhang, W. Wang, B. Han and Q. Chen, *Talanta*, 2015, **144,** 823.
30. T. Winuprasith, S. Chantarak, M. Suphantharika, L. He and D. J. Mcclements, *J. Colloid Interface Sci.*, 2014, **426**, 333.
31. W. Kevin, S. P. Sherlock and D. Hongjie, *Proc. Natl. Acad. Sci. U. S. A.*, 2011, **108**, 8943.